Chinese Journal of
POLYMER SCIENCE

RESEARCH ARTICLE

https://doi.org/10.1007/s10118-023-3007-2
Chinese J. Polym. Sci. **2023**, *41*, 1525–1532

Catalyst-Free Four-Component Spiropolymerization for the Construction of Spirocopolymers with Tunable Photophysical Properties

Luo-Jie Zhu[a,†], Gui-Nan Zhu[a,†], Wen-Ya Yan[a], Peng Sun[b*], Jian-Bing Shi[a], Jun-Ge Zhi[c], Bin Tong[a], Zheng-Xu Cai[a], and Yu-Ping Dong[a*]

[a] *Beijing Key Laboratory of Construction Tailorable Advanced Functional Materials and Green Applications, School of Materials Science and Engineering, Beijing Institute of Technology, Beijing 100081, China*
[b] *Advanced Research Institute of Multidisciplinary Science, Beijing Institute of Technology, Beijing 100081, China*
[c] *Key Laboratory of Cluster Science of Ministry of Education, School of Chemistry and Chemical Engineering, Beijing Institute of Technology, Beijing 100081, China*

Electronic Supplementary Information

Abstract Spiropolymers have gained a great deal of interest from both academic and industrial fields by virtue of their unique geometric structures and physical properties. Herein, we prepared a series of spirocopolymers through the catalyst-free four-component spiropolymerization of diisocyanides, activated alkynes, and two different kinds of monomers with reactive carbonyl groups. It is found that the polymerization reactivity of monomers, feeding modes, and feed ratios play significant roles in spirocopolymerization. Monomers with high reactivity and feeding reactive monomers first contribute to improving the molecular weights and yields of the polymers. The constructed copolymers have two different kinds of spiro structures, which is confirmed by the nuclear magnetic resonance. In addition, the spirocopolymers display the unique cluster-triggered emission and aggregation-induced emission properties, and their emission properties can be well-modulated by altering the ratio of comonomers. It is highly anticipated that this line of research will enrich the methodology of multi-component spiropolymerization, and provide a new insight into developing spiropolymers with various spiro structures and tunable properties.

Keywords Multi-component spiropolymerization; Spirocopolymers; Aggregation-induced emissions; Clusterization-triggered emissions

Citation: Zhu, L. J.; Zhu, G. N.; Yan, W. Y.; Sun, P.; Shi, J. B.; Zhi, J. G.; Tong, B.; Cai, Z. X.; Dong, Y. P. Catalyst-free four-component spiropolymerization for the construction of spirocopolymers with tunable photophysical properties. *Chinese J. Polym. Sci.* **2023**, *41*, 1525–1532.

INTRODUCTION

Spiropolymers are known as polymers containing the spiroring structure in their repeating units, and have drawn broad interest from both academic and industrial communities.[1–5] Their unique chemical structures endow them with high thermal and chemical stability since the opening of spiroring structure will not result in the degradation of polymer chains directly. Spiropolymers also display many unusual properties, such as spiroconjugation, spiro-superconjugation, and heterohead effects, showing promising potentials for use in biomedical and organic photovoltaic fields.[6–10] Generally, strategies for constructing spiropolymers can be divided into two categories: the polymerization of pre-synthesized spiroring monomers and the spiropolymerization of non-spiroring monomers.[5] A series of spiropolymers with the functionalities of gas separation, hydrogen storage, opt-electric conversion, *etc.*, have been successfully fabricated through the polymerization of pre-synthesized spiroring monomers.[11–21] At the same time, a variety of reactions, such as Suzuki-coupling and thiol-ene click reactions, have been applied to polymerize the pre-synthesized spiroring monomer.[22–31]

In recent years, spiropolymers fabricated through the spiropolymerization of non-spiroring monomers have attracted a lot of attention owing to the wide availability of non-spiroring monomers.[32,33] Meanwhile, multi-component reactions have been explored and utilized to construct polymers with complex structures.[34–45] Inspired by the multi-component reaction among isocyanides, alkynes, and the third component,[46–49] our group nominated the multi-component spiropolymerization (MCSP) concept and successfully constructed 1,6-dioxospiro[4.4]nonane-3,8-diene spiropolymers through the three-component polymerization of diisocyanides, activated alkynes, and carbon dioxide without the usage of metal-based catalyst.[5] Since then, a series of spiropolymers with novel chemical structures and unique properties were pre-

* Corresponding authors, E-mail: sunpeng@bit.edu.cn (P.S.)
E-mail: chdongyp@bit.edu.cn (Y.P.D.)
† These authors contributed equally to this work.
Special Issue: Celebrating the 70th Anniversary of the Establishment of Polymer Program at Peking University
Received March 26, 2023; Accepted May 23, 2023; Published online July 5, 2023

pared through the MCSP of diisocyanides, activated alkynes, and monomers containing reactive carbonyl groups. For example, 4,7-bis[alkyl(aryl)imino]-2-phenyl-3-oxa-6-thia-1-azaspiro-[4.4]nona-1,8-dienes spiropolymers were fabricated through the MCSP of diisocyanides, activated alkynes, and benzoyl isothiocyanate. Interestingly, the prepared spiropolymers displayed the cluster-triggered emission (CTE) property resulting from their strong non-covalent interactions with MDM2 protein, showing immense potentials for application in the diagnosis and treatment of tumor cells.[33] In addition, a series of bis-spiropolymers were successfully constructed through the MCSP of diisocyanides, activated alkynes, and halogenated quinones, and these spiropolymers could photodegrade into small-molecule segments after doped with rhodamine B under irradiation with simulated sunlight.[5] Very recently, spiropolymers with intrinsic acid-degradation capability were synthesized through the MCSP of diisocyanides, activated alkynes, and bis-anhydrides.[50] Despite great progress has been made, previous research mainly focuses on the construction of spirohomopolymer, and little attention has been paid in developing spirocopolymers.[17,51] Compared with spirohomopolymers, spirocopolymers have more than one kind of spiroring structures, and could display various unique physical and chemical properties simultaneously. Meanwhile, by altering the variety and ratio of comonomers, the chemical and physical properties of spirocopolymers can be well-modulated. Therefore, the development of spirocopolymer is of vital significance, yet it still remains unexplored.

Herein, we prepared a series of spirocopolymers through the four-component spiropolymerization of diisocyanides, activated alkynes, and two different kinds of monomers containing reactive carbonyl groups. As illustrated in Scheme 1, 1,4-diisocyanocyclohexane, diethyl acetylenedicarboxylate, and 3,3′,4,4′-benzophenonetetracarboxylic dianhydride are chosen as the first, second and third monomers, respectively. Through polymerizing them with the fourth monomer such as benzoyl isothiocyanate, 4,4′-bis(2-bromoacetyl)biphenyl, and 2,5-dichloro-1,4-benzoquinone, a series of spirocopolymers with more than one kind of spiroring structures are successfully constructed. The effect of the polymerization reactivity of monomers, feeding modes, and feed ratios on the spirocopolymerization were investigated. It is found that monomers with high reactivity and feeding reactive monomers first contribute to improving molecular weights and yields. The chemical structures of spirocopolymers were confirmed by ^{1}H-NMR and ^{13}C-NMR spectra. In addition, the prepared spirocopolymers display the CTE and aggregation-induced emission (AIE) properties, and their emission properties can be well-modulated by changing the ratio of comonomers. Therefore, spirocopolymers with tunable photophysical properties are successfully constructed through the four-component spiropolymerization of diisocyanides, activated alkynes, and two different kinds of monomers containing reactive carbonyl groups.

EXPERIMENTAL

Materials

1,4-Diisocyanocyclohexane (**1**) was prepared according to the previous work.[33] Diethyl acetylenedicarboxylate (**2**) and 3,3′,4,4′-benzophenonetetracarboxylic dianhydride (**3a**) were purchased from Energy Chemical. Benzoyl isothiocyanate (**3b**), 4,4′-bis(2-bromoacetyl)biphenyl (**3c**), and 2,5-dichloro-1,4-benzoquinone (**3d**) were purchased from Meryer. Tetrahydrofuran (THF), dichloroethane (DCE) and hexane were purchased from Tianjin Jindong Tianzheng Fine Chemical Reagent Factory. All reagents were used as received without further purification.

Measurements

^{1}H-NMR and ^{13}C-NMR spectra were recorded on a Bruker Avance III 400 spectrometer at room temperature. Gel permeation chromatography (GPC) was performed using a Waters 1515 isocratic high performance liquid chromatography pump and a Waters 2414 refractive index detector. THF was used as the eluent with a flow rate of 1.0 mL/min. The column

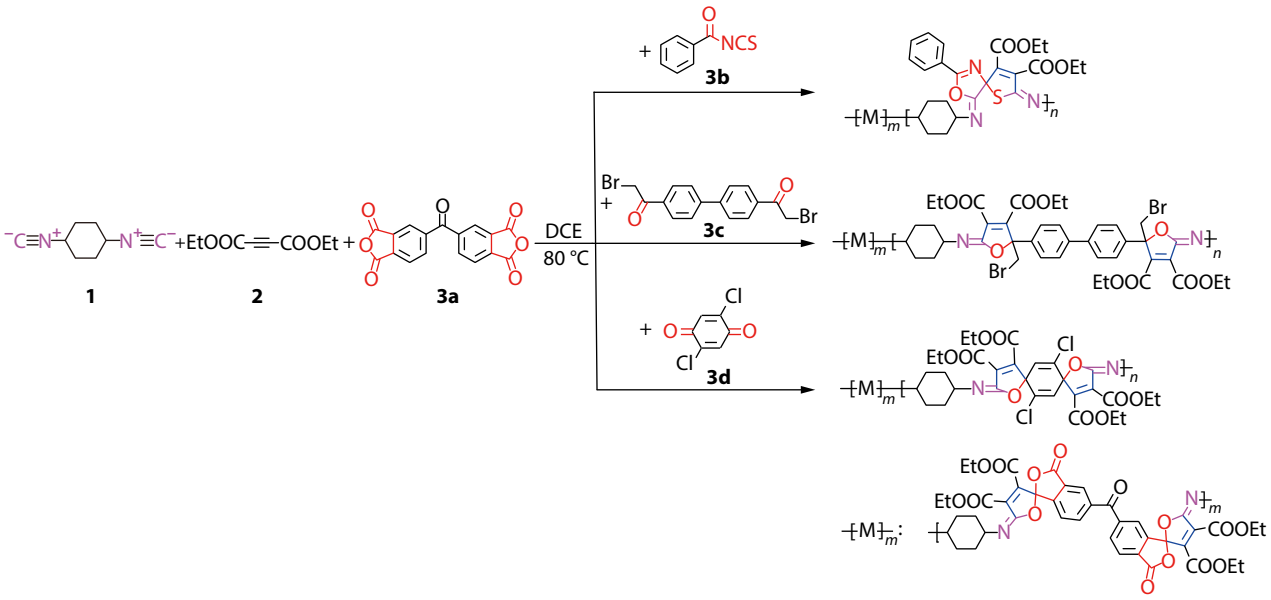

Scheme 1 Synthetic routes to spirocopolymers.

https://doi.org/10.1007/s10118-023-3007-2

temperature was 40 °C and polystyrene standards were used for the calibration. UV-Vis spectra were recorded using a TU-1901 double-beam ultraviolet spectrophotometer. Fluorescence spectra were performed on a Hitachi F-7000 fluorescence spectrophotometer.

Synthetic Procedure of Spirocopolymers

Strategies to construct spirocopolymers are divided into the one-pot and two-step methods. The one-pot strategy is described utilizing spirocopolymer **P2** as an example: monomers **1** (67.0 mg, 0.5 mmol), **2** (170.0 mg, 1.0 mmol), **3a** (80.6 mg, 0.25 mmol), and **3b** (40.8 mg, 0.25 mmol) were added into a 25 mL Schlenk tube and dissolved by 5 mL of DCE. The polymerization was stirred at 80 °C for 6 h under an ambient atmosphere. After the polymerization was finished, the mixture was cooled to room temperature and precipitated into 200 mL of hexane. The same precipitation process was repeated for another time to obtain the neat spirocopolymer. The two-step strategy is described utilizing spirocopolymer **P3** as an example: monomers **1** (67.0 mg, 0.5 mmol), **2** (170.0 mg, 1.0 mmol), and **3a** (80.6 mg, 0.25 mmol) were added into a 25 mL Schlenk tube and dissolved by 5 mL of DCE, and the polymerization was stirred at 80 °C for 3 h. Then monomer **3b** (40.8 mg, 0.25 mmol) was added and stirred for another 3 h in air. After the polymerization was finished, the mixture was cooled to room temperature and precipitated into 200 mL of hexane. The same precipitation process was repeated for another time to obtain the neat spirocopolymer.

RESULTS AND DISCUSSION

Polymerization

To investigate the polymerization reactivity of monomers **3a**–**3d**, the three-component polymerization of monomers **1**, **2**, and **3** was conducted under the same conditions. As shown in Table 1, among prepared spiropolymers, **P-3a** achieves a high yield of 82.5% and the highest number-average molecular weight (M_n) of 8100 simultaneously, which indicates that monomer **3a** displays the highest polymerization reactivity among monomer **3**. Spiropolymer **P-3d** realizes a similar yield of 84.0% but a moderate M_n of 6100, demonstrating that monomer **3d** has a lower polymerization reactivity than that of monomer **3a**. Table 1 also shows that polymer **P-3c** achieves a moderate yield of 72.9% and M_n of 4300, and spiropolymer **P-3b** has a low yield of 66.6% and M_n of 3400. These results indicate that monomer **3c** is more reactive to polymerize with monomers **1** and **2** than monomer **3b**, but less reactive than monomer **3d**. In short, the polymerization reactivity of monomer **3** follows the order: **3a**>**3d**>**3c**>**3b**. In the subsequent discussion, monomer **3a** with the highest polymerization reactivity is chosen as the third component, and monomer **3b**, **3c** and **3d** are chosen as the forth component to construct spirocopolymers, respectively. Compared with our previous studies, polymers **P-3a**–**P-3d** have moderate yields and low molecular weights due to the unoptimized polymerization conditions. The yields and molecular weight can be improved by prolonging polymerization time and increasing monomer concentration.[33,50]

To figure out the effect of feeding mode on spirocopolymerization, spirocopolymers **P2**, **P3** and **P4** were prepared through the four-component polymerization of monomers **1**, **2**, **3a**, and **3b** with the different feeding sequence, respectively. As shown in Table 2, spirocopolymer **P2**, which is constructed through the one-pot strategy, has a moderate yield of 81.6% and M_n of 15400. Interestingly, the yield increases to 89.2% and the M_n increases to 18700 when changing the feeding mode from the one-pot to two-step method, and feeding monomer **3a** prior to **3b**. These results indicate that monomer **3b** displays the high reactivity to polymerize with oligomers formed from monomers **1**, **2**, and **3a**, which contributes to the propagation of copolymer chain. However, Table 2 also shows that the yield decreases sharply to 60.3% and the M_n declines dramatically to 4800 once feeding monomer **3b** prior to **3a**. This phenomenon could result from

Table 1 Three-component polymerization data from the polymerization of monomers **1**, **2**, and **3**.[a]

Entry	Polymers	Monomers	Yield (%)	M_n[b]	$Đ$[b]
1	**P-3a**	**1**+**2**+**3a**	82.5	8100	4.33
2	**P-3b**	**1**+**2**+**3b**	66.6	3400	1.60
3	**P-3c**	**1**+**2**+**3c**	72.9	4300	2.19
4	**P-3d**	**1**+**2**+**3d**	84.0	6100	2.36

[a] Carried out in DCE at 80 °C for 3 h, [**1**] = 0.10 mol/L, [**1**]:[**2**]:[**3**]=1:2:1; [b] Determined by GPC utilizing THF as eluent and linear polystyrenes as the calibration standards. M_n is the number-average molecular weight; $Đ = M_w/M_n$, where M_w is the weight-average molecular weight.

Table 2 Four-component polymerization data from the polymerization of monomers **1**, **2**, **3a**, and **3***.[a]

Entry	Polymers	Feeding sequence and reaction time	[**3a**] (mmol)	[**3***] (mmol)	Yield (%)	M_n[b]	$Đ$[b]
1	**P1**	**3a** 3 h	0.25	–	70.3	6000	2.08
2	**P2**	**3a** + **3b** 6 h	0.25	0.25	81.6	15400	3.11
3	**P3**	**3a** 3 h + **3b** 3 h	0.25	0.25	89.2	18700	3.26
4	**P4**	**3b** 3 h + **3a** 3 h	0.25	0.25	60.3	4800	1.64
5	**P5**	**3a** 3 h + **3b** 3 h	0.10	0.40	84.5	7600	2.00
6	**P6**	**3a** 3 h + **3b** 3 h	0.20	0.30	85.5	14200	2.69
7	**P7**	**3a** 3 h + **3b** 3 h	0.30	0.20	87.4	19600	4.76
8	**P8**	**3a** 3 h + **3b** 3 h	0.40	0.10	86.1	18400	3.04
9	**P9**	**3a** 3h + **3c** 3 h	0.25	0.25	85.8	9500	3.33
10	**P10**	**3a** 3 h + **3d** 3 h	0.25	0.25	92.6	11400	4.44

[a] Carried out in DCE at 80 °C, [**1**]=0.10 mol/L, [**1**]:[**2**]=1:2; [b] Determined by GPC utilizing THF as eluent and linear polystyrenes as the calibration standards. M_n is the number-average molecular weight; $Đ = M_w/M_n$, where M_w is the weight-average molecular weight.

https://doi.org/10.1007/s10118-023-3007-2

that monomer **3a** has low polymerization reactivity with oligomers formed from monomers **1**, **2**, and **3b**. Therefore, all these results demonstrate that the feeding mode plays a significant role in four-component polymerization, and feeding the reactive monomer first contributes to achieving high yield and M_n.

To study the effect of feed ratio on spiropolymerization, spirocopolymers **P5**-**8** were prepared through the four-component polymerization of monomers **1**, **2**, **3a**, and **3b** with the different feed ratio between **3a** and **3b**, respectively. As shown in Table 2, by changing the feed ratio from 1:4 to 2:3 and 1:1, the M_n of prepared spirocopolymer increases significantly from 7600 to 14200, and 18700, respectively. However, when changing the feed ratio from 1:1 to 3:2 and 4:1, the M_n of prepared spirocopolymer remains almost unchanged. Meanwhile, the yield of spirocopolymer always keeps nearly unchanged by changing feed ratio. With the proportion of reactive monomer **3a** increasing, the propagation of polymer chain could be promoted because more monomers **1** and **2** react with monomer **3a**, and participate in the polymerization. Further increase of monomer **3a** does not lead to a higher M_n since the propagation of polymer chain has been controlled and determined by the polymerization reactivity of monomer **3a**. These results show that the feed ratio between the third and fourth component monomers is of importance to the molecular weight, and a high proportion of reactive monomers contributes to improving molecular weights. Additionally, spirocopolymer **P9** was prepared through the four-component polymerization of monomers **1**, **2**, **3a**, and **3c**, and spirocopolymer **P10** was prepared through the four-component polymerization of monomers **1**, **2**, **3a**, and **3d**. The successful construction of **P9** and **P10** indicates that the four-component polymerization is a powerful strategy to construct spirocopolymers, and the chemical structure of spirocopolymer can be well-modulated by altering the kind of comonomers.

Structural Characterization

To confirm the chemical structure of spirocopolymer fabricated through four-component polymerization, ^{1}H-NMR and ^{13}C-NMR spectra of monomers **1**, **2**, and **3b**, and spiropolymers **P-3a**, **P-3b**, and **P3** were performed. Spirocopolymers **P3**, **P9**, and **P10** have similar chemical structures, and **P3** is taken as an example to discuss the key features of four-component polymerization. As shown in Figs. 1(a)–1(d), the characteristic proton resonances of monomers **1**, **2**, and **3b** are all reserved in the ^{1}H-NMR spectra

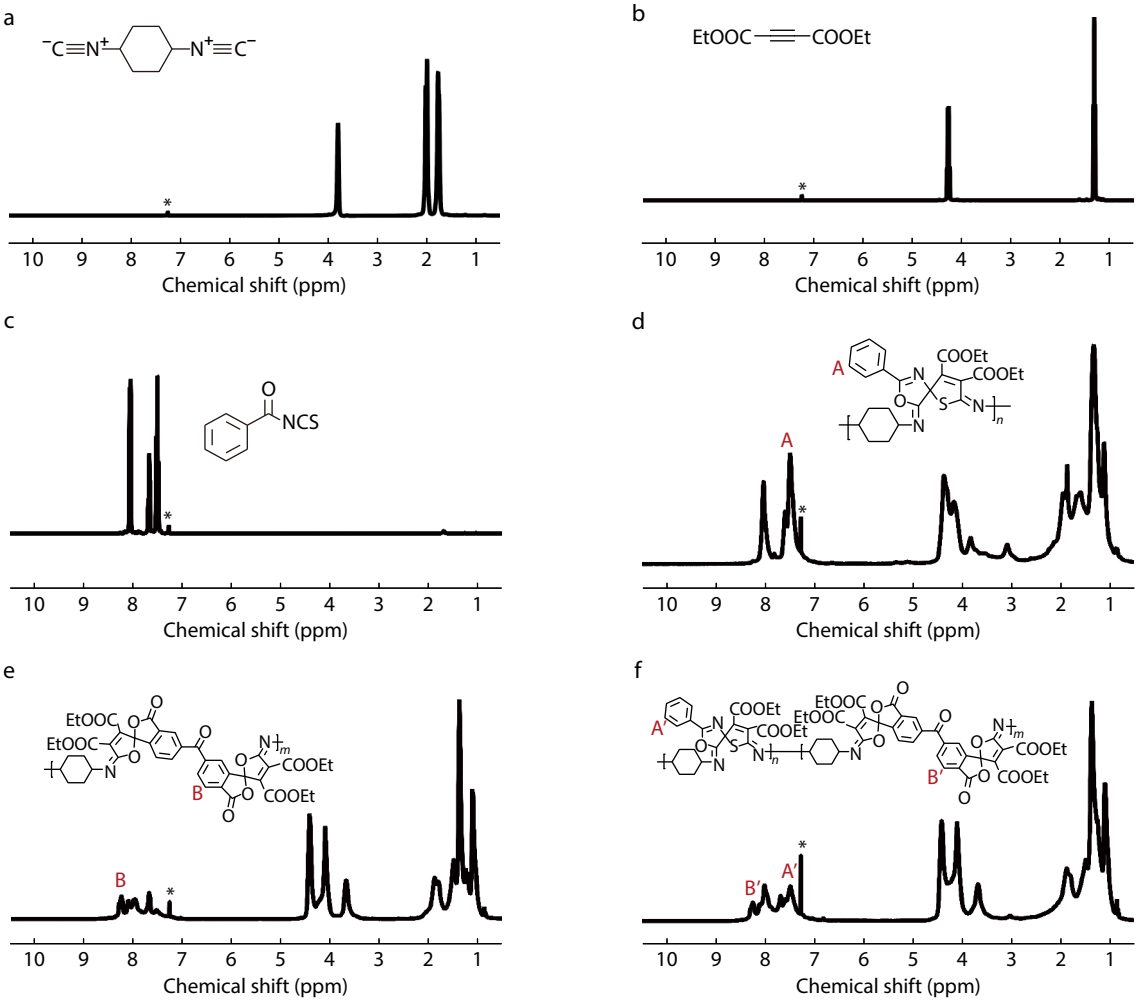

Fig. 1 ^{1}H-NMR spectra of (a) **1**, (b) **2**, (c) **3b**, (d) **P-3b**, (e) **P-3a**, and (f) **P3** in $CDCl_3$. The solvent peaks are marked with asterisks.

https://doi.org/10.1007/s10118-023-3007-2

of **P-3b** with slight chemical shifts after polymerization, which confirms the successful construction of spiropolymer **P-3b**. Figs. 1(d)–1(f) show that both the characteristic H_A of **P-3b** at δ=7.48 ppm and characteristic H_B of **P-3a** at δ=8.25 ppm are present in **P3** as $H_{A'}$ and $H_{B'}$, indicating the successful fabrication of spirocopolymer **P3**.

The chemical structure of spirocopolymer **P3** can be further confirmed by ^{13}C-NMR spectra. As shown in Fig. 2, the resonance signal of monomer **1** at δ=156.91 ppm, that of monomer **2** at δ=77.36 ppm, and that of monomer **3b** at δ=135.09 and 161.71 ppm completely disappear in the ^{13}C-NMR spectra of **P-3b**, **P-3a**, and **P3**, respectively, demonstrating the complete consumption of monomer. In addition, as shown in Figs. 2(d)–2(f), the emerging signal located at δ=84.64 ppm is assigned to the resonance of spirocarbon atom C_A of **P-3b**, and that located at δ=108.91 ppm is assigned to the resonance of spirocarbon atom C_B of **P-3a**. Two similar signals $C_{A'}$ and $C_{B'}$ also appear at the corresponding locations in the ^{13}C-NMR spectra of **P3**, indicating the successful construction of spirocopolymer **P3**. Therefore, all these results confirm that spirocopolymers with two different spiroring structures are successfully constructed through four-component spiropolymerization.

Photophysical Properties

To investigate the photophysical properties of resultant spirocopolymers, the UV-Vis absorption spectra of **P1**–**P10** were collected from their THF solutions. As shown in Figs. 3(a)–3(c), the maximum absorption peaks of **P1**–**P10** appear at around 250 nm, which correspond to the *n*-π^* transition of C=O from ester group and the B-band absorption of phenyl ring. The spirocopolymers also show a distinct absorption band at 380 nm. This absorption band could stem from the conjugation of C=C−C=N in polymer main chains. Moreover, as shown in Fig. 3(b), the absorption band at 380 nm decreases gradually with the proportion of monomer **3a** increasing. The reason behind such phenomenon could result from that spiroring structure formed form monomer **3a** display larger steric hindrance and weaken the conjugation of C=C−C=N among polymer chains. Fluorescence emission spectra of spiropolymers **P1**–**P10** were also collected from their THF solutions. As shown in Figs. 3(d)–3(f), all the spirocopolymers have the capability of emitting fluorescence even at a high concentration of 1.0×10^{-3} mol/L, which confirms their CTE properties. The emission wavelengths of spirocopolymers **P5**–**P8** shift gradually from

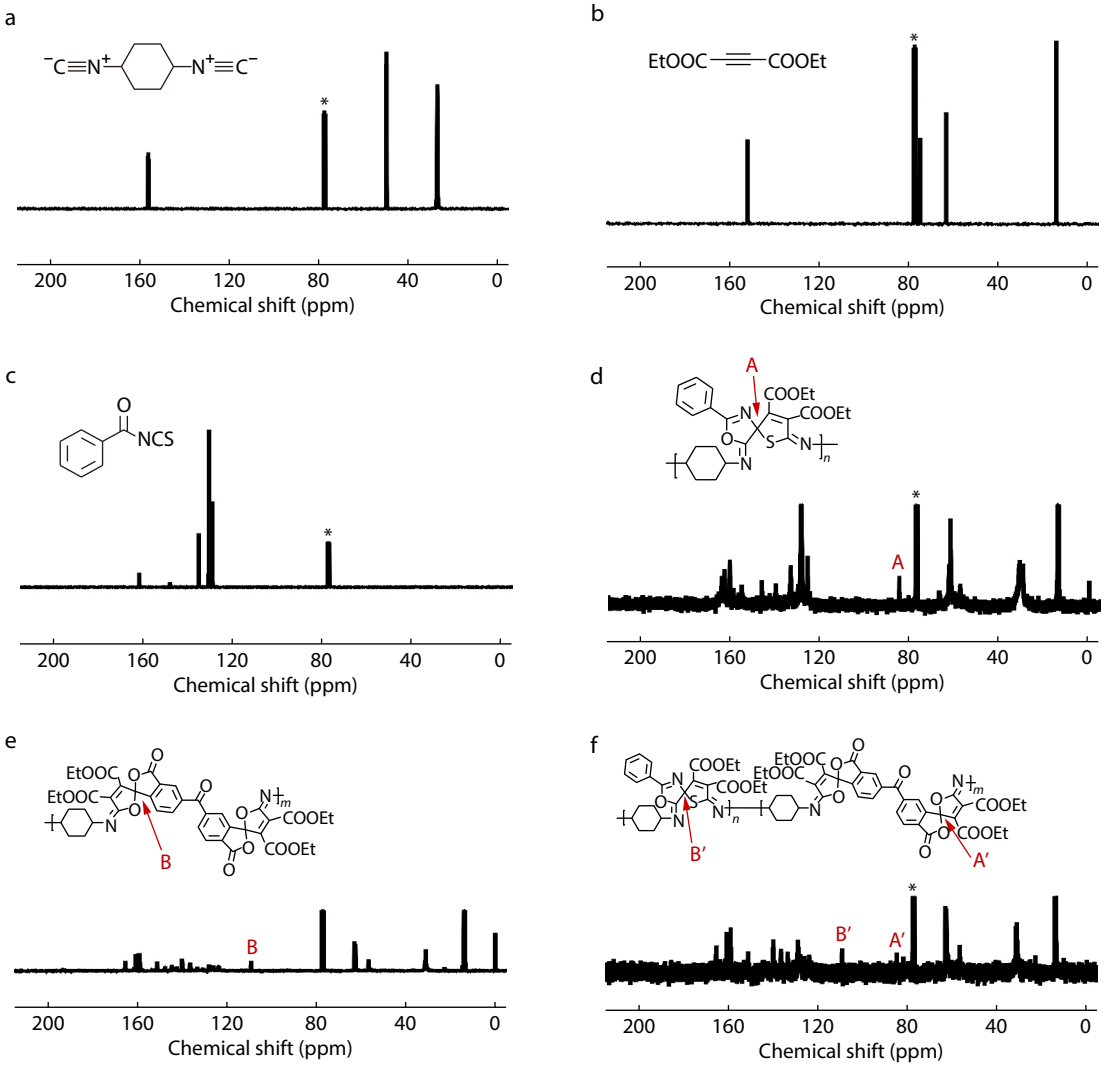

Fig. 2 ^{13}C-NMR spectra of (a) **1**, (b) **2**, (c) **3b**, (d) **P-3b**, (e) **P-3a**, and (f) **P3** in $CDCl_3$. The solvent peaks are marked with asterisks.

https://doi.org/10.1007/s10118-023-3007-2

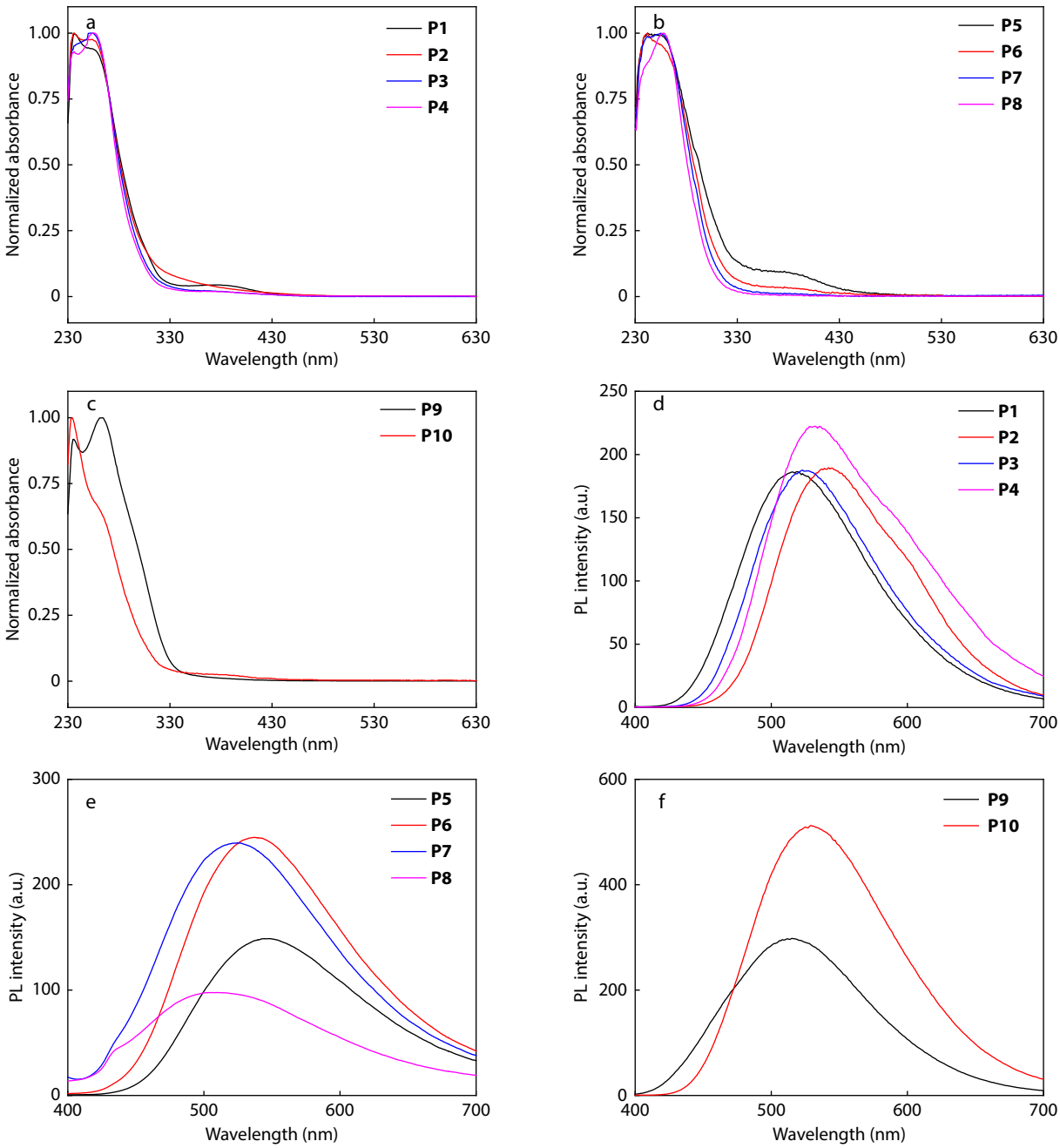

Fig. 3 (a–c) Normalized UV-Vis absorption (1.0×10^{-5} mol/L) and (d–f) fluorescence spectra (1.0×10^{-3} mol/L, λ_{ex}=380 nm) of spiropolymers **P1**–**P10** in their THF solutions.

548 nm to 510 nm with the proportion of monomer **3a** increasing. This change could result from that the spiroring structure formed from monomer **3a** is against the through-space interaction within and among spirocopolymer chains.

To further investigate the CTE and AIE properties of spirocopolymers **P5**–**P8**, their fluorescence emission spectra were collected from their THF solutions with different concentrations, and THF/H_2O solutions with different water fractions. As shown in Fig. 4(a), with the concentration increasing, the fluorescence intensity of spirocopolymer firstly increases and then decreases, changing in a concentration-dependent manner. This result further confirms the CTE properties of spirocopolymers. Fig. 4(b) shows that the fluorescence intensities of spirocopolymers **P5**–**P8** increase gradually with the water fraction increasing, which demonstrates their AIE properties. In addition, Figs. 4(a) and 4(b) show that spirocopolymer **P5** usually exhibits a higher fluorescence intensity than those of spirocopolymers **P6**, **P7** and **P8**. This result indicates that the spirocopolymer with a high proportion of monomer **3b** could have a better luminescent property. Therefore, all of results confirm that the developed spirocopolymer displays both CTE and AIE properties, and its photophysical property can be well-modulated by changing the ratio of comonomers.

https://doi.org/10.1007/s10118-023-3007-2

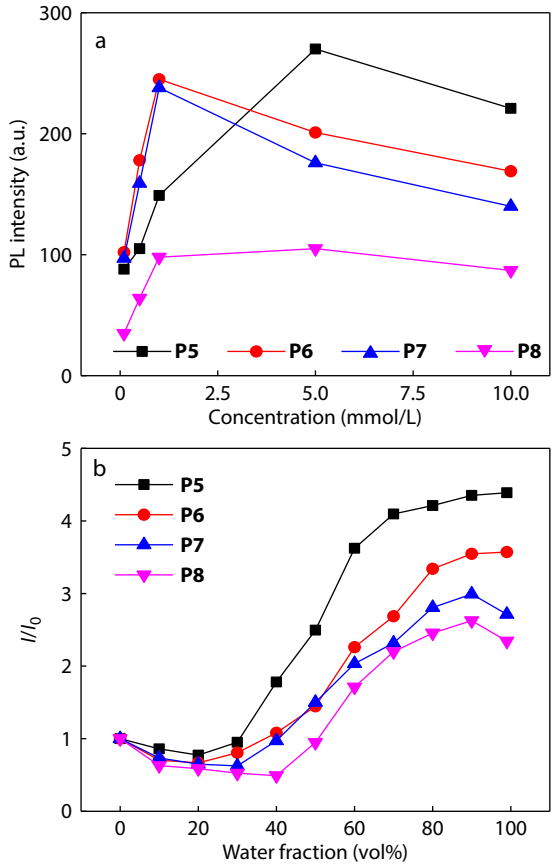

Fig. 4 (a) CTE behavior of spirocopolymers **P5**–**P8** in THF (λ_{ex}= 380 nm); (b) AIE behavior of spirocopolymers **P5**–**P8** in THF/H_2O system (λ_{ex}=380 nm, 5.0×10^{-4} mol/L).

CONCLUSIONS

In summary, we successfully prepared a series of spirocopolymers through the four-component polymerization of diisocyanides, activated alkynes, and two different monomers with reactive carbonyl groups. Monomers with high polymerization reactivity and feeding the reactive monomer first contribute to realizing high molecular weights and yields of polymers. The key structural features of spiro copolymers are verified by the NMR technique. In addition, the constructed spiro copolymers display both CTE and AIE characteristics, and their emission properties can be well-modulated by changing the ratio of comonomers. It is highly anticipated that this line of research will open a new avenue of developing spiropolymers with various spiro structures and tunable properties.

Conflict of Interests

The authors declare no interest conflict.

Electronic Supplementary Information

Electronic supplementary information (ESI) is available free of charge in the online version of this article at http://doi.org/10.1007/s10118-023-3007-2.

ACKNOWLEDGMENTS

This work was financially supported by the National Natural Science Foundation of China (Nos. 21875019, 22175023, 21975020 and 21975021), the National Key Research and Development Program of China (No. 2018YFA0901800) College Students' Innovative Entrepreneurial Training Plan Program (No. BIT2022LH180) and Beijing Institute of Technology Research Fund Program for Young Scholars.

REFERENCES

1 Liaw, D. J.; Wang, K. L.; Huang, Y. C.; Lee, K. R.; Lai, J. Y.; Ha, C. S. Advanced polyimide materials: syntheses, physical properties and applications. *Prog. Polym. Sci.* **2012**, *37*, 907–974.
2 Pham, T. H.; Olsson, J. S.; Jannasch, P. N-spirocyclic quaternary ammonium ionenes for anion-exchange membranes. *J. Am. Chem. Soc.* **2017**, *139*, 2888–2891.
3 Han, T.; Yao, Z.; Qiu, Z.; Zhao, Z.; Wu, K.; Wang, J.; Poon, A. W.; Lam, J. W. Y.; Tang, B. Z. Photoresponsive spiro-polymers generated *in situ* by C–H-activated polyspiroannulation. *Nat. Commun.* **2019**, *10*, 5483.
4 Thompson, K. A.; Mathias, R.; Kim, D.; Kim, J.; Rangnekar, N.; Johnson, J. R.; Hoy, S. J.; Bechis, I.; Tarzia, A.; Jelfs, K. E.; McCool, B. A.; Livingston, A. G.; Lively, R. P.; Finn, M. G. N-aryl-linked spirocyclic polymers for membrane separations of complex hydrocarbon mixtures. *Science* **2020**, *369*, 310–315.
5 Cai, Z.; Ren, Y.; Li, X.; Shi, J.; Tong, B.; Dong, Y. Functional isocyanide-based polymers. *Acc. Chem. Res.* **2020**, *53*, 2879–2891.
6 Wang, M.; Li, C.; Lv, A.; Wang, Z.; Bo, Z. Spirobifluorene-based conjugated polymers for polymer solar cells with high open-circuit voltage. *Macromolecules* **2012**, *45*, 3017–3022.
7 Wang, X.; Zhao, L.; Shao, S.; Ding, J.; Wang, L.; Jing, X.; Wang, F. Poly(spirobifluorene)s containing nonconjugated diphenylsulfone moiety: toward blue emission through a weak charge transfer effect. *Macromolecules* **2014**, *47*, 2907–2914.
8 Valero, S.; Collavini, S.; Völker, S. F.; Saliba, M.; Tress, W. R.; Zakeeruddin, S. M.; Grätzel, M.; Delgado, J. L. Dopant-free hole-transporting polymers for efficient and stable perovskite solar cells. *Macromolecules* **2019**, *52*, 2243–2254.
9 Ma, J.; Tian, J.; Liu, Z.; Shi, D.; Zhang, X.; Zhang, G.; Zhang, D. Multi-stimuli-responsive field-effect transistor with conjugated polymer entailing spiropyran in the side chains. *CCS Chem.* **2019**, *1*, 632–641.
10 Vidavsky, Y.; Yang, S. J.; Abel, B. A.; Agami, I.; Diesendruck, C. E.; Coates, G. W.; Silberstein, M. N. Enabling room-temperature mechanochromic activation in a glassy polymer: synthesis and characterization of spiropyran polycarbonate. *J. Am. Chem. Soc.* **2019**, *141*, 10060–10067.
11 Wu, Y.; Zhang, J.; Fei, Z.; Bo, Z. Spiro-bridged ladder-type poly(*p*-phenylene)s: towards structurally perfect light-emitting materials. *J. Am. Chem. Soc.* **2008**, *130*, 7192–7193.
12 Jiang, J.-X.; Laybourn, A.; Clowes, R.; Khimyak, Y. Z.; Bacsa, J.; Higgins, S. J.; Adams, D. J.; Cooper, A. I. High surface area contorted conjugated microporous polymers based on spirobipropylenedioxythiophene. *Macromolecules* **2010**, *43*, 7577–7582.
13 Bezzu, C. G.; Carta, M.; Tonkins, A.; Jansen, J. C.; Bernardo, P.; Bazzarelli, F.; McKeown, N. B. A spirobifluorene-based polymer of intrinsic microporosity with improved performance for gas separation. *Adv. Mater.* **2012**, *24*, 5930–5933.
14 Ma, X.; Salinas, O.; Litwiller, E.; Pinnau, I. Novel spirobifluorene- and dibromospirobifluorene-based polyimides of intrinsic microporosity for gas separation applications. *Macromolecules* **2013**, *46*, 9618–9624.
15 Zhao, Y. C.; Zhang, L. M.; Wang, T.; Han, B. H. Microporous organic polymers with acetal linkages: synthesis, characterization, and

gas sorption properties. *Polym. Chem.* **2014**, *5*, 614–621.
16 Shamsipur, H.; Dawood, B. A.; Budd, P. M.; Bernardo, P.; Clarizia, G.; Jansen, J. C. Thermally rearrangeable PIM-polyimides for gas separation membranes. *Macromolecules* **2014**, *47*, 5595–5606.
17 McDowell, J. J.; Gao, D.; Seferos, D. S.; Ozin, G. Synthesis of poly(spirosilabifluorene) copolymers and their improved stability in blue emitting polymer LEDs over non-spiro analogs. *Polym. Chem.* **2015**, *6*, 3781–3789.
18 Olsson, J. S.; Pham, T. H.; Jannasch, P. Poly(*N*,*N*-diallylazacycloalkane)s for anion-exchange membranes functionalized with *N*-spirocyclic quaternary ammonium cations. *Macromolecules* **2017**, *50*, 2784–2793.
19 Nagatsu, G.; Sakanoue, T.; Tane, S.; Yonekawa, F.; Takenobu, T. An ester-substituted polyfluorene derivative for light-emitting electrochemical cells: bright blue emission and its application in a host–guest system. *Mater. Chem. Front.* **2018**, *2*, 952–958.
20 Xu, X.; Li, X.; Wang, S.; Ding, J.; Wang, L. Deep-blue emitting poly[spiro(dibenzoazasiline-10',9-silafluorene)] for power-efficient PLEDs. *J. Mater. Chem. C* **2018**, *6*, 9599–9606.
21 Foster, A. B.; Tamaddondar, M.; Luque-Alled, J. M.; Harrison, W. J.; Li, Z.; Gorgojo, P.; Budd, P. M. Understanding the topology of the polymer of intrinsic microporosity PIM-1: cyclics, tadpoles, and network structures and their impact on membrane performance. *Macromolecules* **2020**, *53*, 569–583.
22 Pemba, A. G.; Rostagno, M.; Lee, T. A.; Miller, S. A. Cyclic and spirocyclic polyacetal ethers from lignin-based aromatics. *Polym. Chem.* **2014**, *5*, 3214–3221.
23 Okuda, H.; Koyama, Y.; Uchida, S.; Michinobu, T.; Sogawa, H.; Takata, T. Reversible transformation of a one-handed helical foldamer utilizing a planarity-switchable spacer and C2-chiral spirobifluorene units. *ACS Macro Lett.* **2015**, *4*, 462–466.
24 K, S. N.; Azechi, M.; Endo, T. Synthesis and properties of spiro-centered benzoxazines. *Macromolecules* **2015**, *48*, 7466–7472.
25 Zhao, Y. C.; Wang, T.; Zhang, L. M.; Cui, Y.; Han, B. H. Microporous spiro-centered poly(benzimidazole) networks: preparation, characterization, and gas sorption properties. *Polym. Chem.* **2015**, *6*, 748–753.
26 Modak, A.; Maegawa, Y.; Goto, Y.; Inagaki, S. Synthesis of 9,9'-spirobifluorene-based conjugated microporous polymers by $FeCl_3$-mediated polymerization. *Polym. Chem.* **2016**, *7*, 1290–1296.
27 Sycks, D. G.; Safranski, D. L.; Reddy, N. B.; Sun, E.; Gall, K. Tough semicrystalline thiol-ene photopolymers incorporating spiroacetal alkenes. *Macromolecules* **2017**, *50*, 4281–4291.
28 Schmidt, S. B.; Kempe, F.; Brügner, O.; Walter, M.; Sommer, M. Alkyl-substituted spiropyrans: electronic effects, model compounds and synthesis of aliphatic main-chain copolymers. *Polym. Chem.* **2017**, *8*, 5407–5414.
29 Feng, Q. Y.; Li, B.; Zuo, Z. Y.; Xie, S. L.; Yu, M. N.; Liu, B.; Wei, Y.; Xie, L. H.; Xia, R. D.; Huang, W. A comparison study of physicochemical properties and stabilities of H-shaped molecule and the corresponding polymer. *Chinese J. Polym. Sci.* **2019**, *37*, 11–17.
30 Fang, L.; Zhou, J.; He, C.; Tao, Y.; Wang, C.; Dai, M.; Wang, H.; Sun, J.; Fang, Q. Understanding how intrinsic micro-pores affect the dielectric properties of polymers: an approach to synthesize ultra-low dielectric polymers with bulky tetrahedral units as cores. *Polym. Chem.* **2020**, *11*, 2674–2680.
31 Tan, W. Y.; Jian, L. F.; Chen, W. P.; Zhang, Y. W.; Lu, X. C.; Huang, W. J.; Zhang, J. S.; Wu, J. W.; Feng, J. L.; Liu, Y. D.; Cui, T. T.; Min, Y. G. A facile strategy for intrinsic low-D_k and low-D_f polyimides enabled by spirobifluorene groups. *Chinese J. Polym. Sci.* **2023**, *41*, 288–296.
32 Fu, W. Q.; Zhu, G. N.; Shi, J. B.; Tong, B.; Cai, Z. X.; Dong, Y. P. Synthesis and properties of photodegradable poly(furan-amine)s by a catalyst-free multicomponent cyclopolymerization. *Chinese J. Polym. Sci.* **2019**, *37*, 981–989.
33 Liu, P.; Fu, W.; Verwilst, P.; Won, M.; Shin, J.; Cai, Z.; Tong, B.; Shi, J.; Dong, Y.; Kim, J. S. MDM2-associated clusterization-triggered emission and apoptosis induction effectuated by a theranostic spiropolymer. *Angew. Chem. Int. Ed.* **2020**, *59*, 8435–8439.
34 Deng, X. X.; Li, L.; Li, Z. L.; Lv, A.; Du, F. S.; Li, Z. C. Sequence regulated poly(ester-amide)s based on passerini reaction. *ACS Macro Lett.* **2012**, *1*, 1300–1303.
35 Han, T.; Deng, H.; Qiu, Z.; Zhao, Z.; Zhang, H.; Zou, H.; Leung, N. L. C.; Shan, G.; Elsegood, M. R. J.; Lam, J. W. Y.; Tang, B. Z. Facile multicomponent polymerizations toward unconventional luminescent polymers with readily openable small heterocycles. *J. Am. Chem. Soc.* **2018**, *140*, 5588–5598.
36 Zhang, J.; Wu, Y. H.; Wang, J. C.; Du, F. S.; Li, Z. C. Functional poly(ester-amide)s with tertiary ester linkages *via* the passerini multicomponent polymerization of a dicarboxylic acid and a diisocyanide with different electron-deficient ketones. *Macromolecules* **2018**, *51*, 5842–5851.
37 Wu, X.; Lin, H.; Dai, F.; Hu, R.; Tang, B. Z. Functional polyselenoureas for selective gold recovery prepared from catalyst-free multicomponent polymerizations of elemental selenium. *CCS Chem.* **2020**, *2*, 191–202.
38 Liu, X.; Xiao, M.; Xue, K.; Li, M.; Liu, D.; Wang, Y.; Yang, X.; Hu, Y.; Kwok, R. T. K.; Qin, A.; Zhu, C.; Lam, J. W. Y.; Tang, B. Z. Heteroaromatic hyperbranched polyelectrolytes: multicomponent polyannulation and photodynamic biopatterning. *Angew. Chem. Int. Ed.* **2021**, *60*, 19222–19231.
39 Wu, X.; He, J.; Hu, R.; Tang, B. Z. Room-temperature metal-free multicomponent polymerizations of elemental selenium toward stable alicyclic poly(oxaselenolane)s with high refractive index. *J. Am. Chem. Soc.* **2021**, *143*, 15723–15731.
40 Zhang, J.; Zang, Q.; Yang, F.; Zhang, H.; Sun, J. Z.; Tang, B. Z. Sulfur conversion to multifunctional poly(*O*-thiocarbamate)s through multicomponent polymerizations of sulfur, diols, and diisocyanides. *J. Am. Chem. Soc.* **2021**, *143*, 3944–3950.
41 Li, M.; Duan, X.; Jiang, Y.; Sun, X.; Xu, X.; He, J.; Zheng, Y.; Song, W.; Zheng, N. Three-component asymmetric polymerization toward chiral polymer. *CCS Chem.* **2022**, *4*, 3402–3415.
42 Li, M.; Fu, X.; Wang, J.; Qin, A.; Tang, B. Z. Progress in isocyanide-based step-growth polymerization. *Macromol. Chem. Phys.* **2022**, *224*, 2200352.
43 Ren, Y.; Dai, W.; Guo, S.; Dong, L.; Huang, S.; Shi, J.; Tong, B.; Hao, N.; Li, L.; Cai, Z.; Dong, Y. Clusterization-triggered color-tunable room-temperature phosphorescence from 1,4-dihydropyridine-based polymers. *J. Am. Chem. Soc.* **2022**, *144*, 1361–1369.
44 Yan, H.; He, Y.; Wang, D.; Han, T.; Tang, B. Z. Aggregation-induced emission polymer systems with circularly polarized luminescence. *Aggregate* **2023**, *4*, e331.
45 Fu, X.; Qin, A.; Tang, B. Z. X-yne click polymerization. *Aggregate* **2023**, *4*, e350.
46 Nair, V.; Vinod, A. U.; Nair, J. S.; Sreekanth, A. R.; Rath, N. P. The reaction of cyclohexyl isocyanide and dimethyl acetylenedicarboxylate with *o*- and *p*-quinones: a novel synthesis of iminolactones. *Tetrahedron Lett.* **2000**, *41*, 6675–6679.
47 Nair, V.; Vinod, A. U.; Abhilash, N.; Menon, R. S.; Santhi, V.; Varma, R. L.; Viji, S.; Mathew, S.; Srinivas, R. Multicomponent reactions involving zwitterionic intermediates for the construction of heterocyclic systems: one pot synthesis of aminofurans and iminolactones. *Tetrahedron* **2003**, *59*, 10279–10286.
48 Yavari, I.; Djahaniani, H. One-step synthesis of substituted 4,7-bis[alkyl(aryl)imino]-3-oxa-6-thia-1-azaspiro[4.4]nona-1,8-dienes. *Tetrahedron Lett.* **2005**, *46*, 7491–7493.
49 Nair, V.; Menon, R. S. Nucleophile-initiated catalytic and multicomponent reactions. *Chem. Rec.* **2019**, *19*, 347–361.
50 Zhu, G.; Lin, N.; Wu, X.; Shi, J.; Tong, B.; Cai, Z.; Zhi, J.; Dong, Y. Multicomponent spiropolymerization of diisocyanides, activated alkynes, and bis-anhydrides. *Macromolecules* **2022**, *55*, 6150–6159.
51 Zhang, J.; Jin, J.; Cooney, R.; Fu, Q.; Qiao, G. G.; Thomas, S.; Merkel, T. C. Synthesis of perfectly alternating copolymers for polymers of intrinsic microporosity. *Polym. Chem.* **2015**, *6*, 5003–5008.

https://doi.org/10.1007/s10118-023-3007-2